

1 **Plate Tectonics and Net Lithosphere Rotation over the past 150 My**

2 Trond H. Torsvik^{1-3*}, Bernhard Steinberger^{4,1,2}, Michael Gurnis⁵, Carmen Gaina^{2,1}

3 ¹Physics of Geological Processes & Geosciences, University of Oslo, Norway

4 ²Centre for Geodynamics, NGU, Trondheim, Norway

5 ³School of Geosciences, University of the Witwatersrand, Johannesburg, South Africa

6 ⁴Helmholtz Centre Potsdam, German Research Centre for Geosciences, Potsdam, Germany

7 ⁵Seismological Laboratory, California Institute of Technology, Pasadena, California, USA

8 *email: t.h.torsvik@fys.uio.no

9

10 **ABSTRACT**

11 We have developed an improved model of global digital palaeo-plate boundaries and plate
12 motion to describe the distribution and history of plates since the Late Jurassic. From this
13 history we computed net lithospheric rotation (NR) through time confirming the so-called
14 westward, but only for the past 30 Myrs. The NR has significantly smaller magnitudes
15 ($0.13^\circ/\text{My}$, past 5 My) than for some other plate models; it averages to $0.11 \pm 0.03^\circ/\text{My}$ for
16 the past 50 My with a small but systematic increase toward the present. The westward drift,
17 seen only for the past 30 My, is attributed to the increased dominance of a steadily growing
18 and accelerating Pacific plate. NR shows peaks with time but only an Early Tertiary peak of
19 $0.33^\circ/\text{My}$ (when the Indian plate was undergoing the largest known acceleration/deceleration)
20 can be interpreted with some confidence. We find a linear decreasing trend in net rotation
21 over the past 150 My, but attribute this trend to increasing reconstruction uncertainties back
22 in time, as subduction consumed more than half of the oceanic crust since the Jurassic. After
23 removing a linear time-trend, we find a NR average of about $0.12^\circ/\text{My}$ for the past 150 My.

24

25 *Keywords:* Plate tectonics, global palaeo-plate boundaries, net lithosphere rotation,
26 westward drift

27

28 **1. Introduction**

29 During the 20th century our description of the movement and deformation of the Earth's outer
30 rigid layer evolved from the hypothesis of Continental Drift (Wegener 1915) into Sea-Floor
31 Spreading (Hess 1962) and to the theory of Plate Tectonics (Wilson 1965, McKenzie &
32 Parker 1967, Morgan 1968, Le Pichon 1968). Now a fourth shift is underway in which Plate
33 Tectonics is being subsumed into a new Mantle Dynamics framework that requires plate

34 motion reconstructions through time to include not only improved relative plate motions but
35 also refined plate motions with respect to the mantle.

36

37 By combining relative and absolute plate motion frames from the Indo-Atlantic (Torsvik et
38 al. 2008a; Steinberger & Torsvik 2008) and the Pacific (Steinberger & Gaina 2008) realms
39 we have re-constructed first order palaeo-plate boundaries for the last 150 Ma. Based on the
40 absolute plate motion frames (Table 1) and guided by numerous regional relative plate
41 tectonic models (oceanic domains mostly summarized by Müller et al. 2008), we developed a
42 global model of “tectonic plates polygons” for each 10 Myr interval since Late Jurassic (150
43 Ma). The plate polygons are closed polygons that outline a rigid block (tectonic plate) that
44 has moved relative to neighboring rigid blocks for a finite amount of time as indicated by the
45 type of the plate boundary between them (see Section 2). This global model can be used for
46 many purposes in geodynamic modeling. Here we describe a single important example,
47 namely the calculation of net lithosphere rotation (NR). If mantle convection is the principal
48 driving mechanism for plate motions, NR should be zero unless individual lithospheric plates
49 have different couplings to the underlying mantle flow. **A proper reference frame with
50 appropriate NR is important for discussions of poloidal/toroidal partitioning of plate motions
51 (Lithgow-Bertelloni et al. 1993).** Most plate models predict westward drift of the lithosphere
52 with respect to the deep mantle, which has been ascribed to lateral viscosity variations
53 (Ricard et al. 1991; O’Connell et al. 1991). Westward drift estimates vary considerably (1.5-
54 9 cm/year) and are usually larger than those calculated from geodynamic models (Becker
55 2006). **However, comparison of westward drift estimates with geodynamic models is
56 problematic, since all geodynamic models are based on simplifying assumptions. Recently,
57 seismic anisotropy has emerged as a further tool to estimate NR for recent times (Becker
58 2008; Kreemer 2009; Conrad & Behn, submitted *Geochem. Geophys. Geosyst.*).** In Section
59 3 we explore NR, not only for present times but for the past 150 Ma.

60

61 **2. Global Plate Polygons**

62 Building global plate polygons through Earth history (Fig. 1; **online supplement**) requires
63 knowledge of relative plate motions from both continental and oceanic areas. The
64 uncertainty in constraining these motions increases for older times, due to the destruction
65 (through subduction) or distortion (such as collision) of relative motion. For example, more
66 than half of the oceanic crust created since the Jurassic has been consumed by subduction,

67 therefore past plate boundary configuration has to be restored by making assumptions based
68 on limited geological constraints (like the age of preserved ophiolites or slab-window related
69 volcanism) and the rules of plate tectonics. **World uncertainty – the fraction of the Earth's**
70 **lithosphere which has been subducted since a given time, and for which plate motion at that**
71 **time is therefore uncertain, reaches ~60% at around 140 Ma (Fig. 2b).**

72

73 Starting with a simplified version of today's tectonic plate boundaries (mostly compiled from
74 Bird 2003), plate polygons were constructed for each 10 Myrs with averaged Euler stage
75 poles computed for 10 Myrs intervals. Polygons were originally constructed using GPlates
76 (Boyden et al. 2010), partly using the continuously closing plate method (Gurnis et al. 2010)
77 and subsequently modified and refined in Arc-GIS. The polygon boundaries and stage poles
78 (online supplement) are based on a large number of sources but a large proportion originate
79 from work by the Geodynamic Teams at NGU & PGP, Norway and the University of Sydney
80 EarthByte Group, Australia (e.g. Alvey et al. 2008, Gaina et al. 1998, 2002, 2009, Gaina &
81 Müller 2007; Heine et al. 2004; Müller et al. 2008; Torsvik et al. 2008a-b, 2009 *and*
82 *references therein*).

83

84 In addition to the traditional plate polygon boundaries (ridge, trench and transform faults) we
85 also include plate boundaries for rifts (divergent 'diffuse' boundaries) where we have been
86 able to quantify the amount of rifting with some confidence. As an example, our 60 Ma
87 reconstruction (Fig. 1b) treats Europe (plate number 301) as a distinct plate (i.e. not attached
88 to Greenland, plate number 102, as it might be deduced from a pre-breakup configuration).
89 At this time, although seafloor spreading was taking place in the Labrador Sea (between
90 Greenland, together with SW Ellesmere and Devon Island, and North America) significant
91 Late Cretaceous-Early Tertiary rifting also took place between East Greenland and NW
92 Europe, and therefore a plate boundary between Greenland and Europe is incorporated to
93 model this rifting. Similarly, at 100 Ma (Fig. 1c), Greenland is kept as a separate plate due to
94 pre-drift rifting versus both North America and Europe. At this time Africa is also divided
95 into three plates (plate numbers 701, 714-715) due to the minor intra-plate Cretaceous rifts
96 that were active at this time. At 150 Ma (Fig. 1d), we combine most of South America and
97 Africa as one plate ('Africa' 701) whilst Patagonia is treated as a separate plate (Torsvik et al.
98 2009). At this time we also combine East Antarctica (802), India (501), Madagascar (702)
99 and Australia as one plate ('Australia' 801).

100

101 We stress that knowledge and data quality differs greatly for smaller areas, from excellent to
 102 poorly constrained, and many plate polygons can only be regarded as provisional. Some
 103 areas are heavily oversimplified (work in progress), but due to the relative small areas
 104 covered by **some of these plates (e.g. within the Caribbean)**, revised boundaries will introduce
 105 only minor differences in the calculations of net lithosphere rotation (Section 3) or derivative
 106 geodynamic modeling.

107

108 **3. Net Lithosphere Rotation**

109 **We computed net rotation of the entire lithosphere as:**

$$110 \mathbf{\omega}_{\text{net}} = 3/(8 \pi r^4) \int \mathbf{v} \times \mathbf{r} dS = 3/(8 \pi r^4) \sum_i \int (\mathbf{\omega}_i \times \mathbf{r}) \times \mathbf{r} dS_i,$$

111 **where \mathbf{v} is the velocity vector, $\mathbf{\omega}_i$ is the rotation rate vector of plate i , \mathbf{r} is the position vector ,**
 112 **$\int \dots dS$ indicates integration over the entire sphere, \sum_i indicates summation over all plates, and**
 113 **$\int \dots dS_i$ indicates integration over the area of plate i .**

114

115 Figure 2b and Table 2 summarize NR calculations through geological time given our plate
 116 rotations and boundaries. We find $0.13^\circ/\text{My}$ for the past 5 Ma, $0.14^\circ/\text{My}$ for the past 10 Ma
 117 and $0.11 \pm 0.03^\circ/\text{My}$ for the past 50 My ($N=5$; **mean and standard deviation of 10 Myr**
 118 **intervals**). These are compatible with the NR estimates by Gordon & Jurdy (1986;
 119 $0.114^\circ/\text{Myr}$), Torsvik et al. (2008a; $0.165^\circ/\text{Myr}$ for the past 5 Myr), and are only slightly
 120 higher than those obtained from numerical computations ($\sim 0.02\text{-}0.11^\circ/\text{My}$; orange ovals in
 121 Fig 2b; Becker 2006) **and also compatible with NR estimates using seismic anisotropy:**
 122 **Becker (2008) finds that only NR up to $\sim 0.2^\circ/\text{Myr}$ is consistent with seismic anisotropy**
 123 **constrained by surface waves. By considering SKS splitting observations, Kreemer (2009)**
 124 **determines a best-fit NR of $0.2065^\circ/\text{Myr}$ around a pole at 57.6°S , 63.2°E . Building upon**
 125 **both these works, Conrad & Behn (manuscript submitted *Geochem. Geophys. Geosyst.*)**
 126 **jointly constrain lithosphere NR and upper mantle viscosity and find that NR should not**
 127 **exceed $0.26^\circ/\text{Myr}$. Our NR vectors differ somewhat compared with previous studies; we**
 128 **obtain higher Euler latitudes (Fig. 4) and thus yielding a more well-defined westward velocity**
 129 **field for the past 30 million years (Fig. 3). The orientation of the axis of net rotation through**
 130 **time, computed here in a mantle reference frame (Fig. 4) also bears considerable resemblance**
 131 **to the no-torque reference frames of Čadež and Ricard (1992; their figs. 4 and 5).**

132

133 Most plate models predict westward drift of varying magnitude; our model estimation has a
134 westward drift at the equator of ~ 1.5 cm/year, but ~ 3 times lower than the 'young' hotspot
135 model of Gripp & Gordon (2002; HS3 in Fig. 2b) and 3-6 times lower than those values
136 estimated by Doglioni (2005) using alternative reference frames. The HS3 model is widely
137 used and discussed in the recent geodynamic literature (e.g. Becker 2006; 2008; Funicello et
138 al. 2008; Husson et al. 2008) but differs from all other plate models in the sense that Africa
139 and Eurasia (for example) are moving south-westward, i.e. opposite to our velocity fields
140 (Fig. 1a; Table 1). **No tracks on the African plate were used to construct the HS3 model.**
141 Morgan & Morgan (2007) have pointed out that the HS3 model yield a too high velocity for
142 the Pacific plate ($1.06^\circ/\text{Myr}$ around a pole of 61.5°S , 90.3°E). Our model when averaged
143 over the last 10 Myr gives a $\sim 20\%$ lower velocity for the Pacific ($0.85^\circ/\text{Myr}$ around a pole of
144 72.6°S , 116.3°E ; **online supplement Table S1**). This is $\sim 6\%$ higher than the model of Morgan
145 and Morgan (2007) with $0.80^\circ/\text{Myr}$ around a pole of 59.3°S , 94.6°E , **$\sim 10\%$ higher than the**
146 **T22A model of Wang & Wang (2001) with $0.775^\circ/\text{Myr}$ around a pole of 63.1°S , 103.9°E ,**
147 **and substantially higher than Pacific plate motions in a no-net rotation frame (e.g., Argus &**
148 **Gordon, 1991; Kreemer & Holt, 2001).**

149

150 Calculating NR through time we find a fluctuating pattern superimposed on a long term
151 descending linear trend since 150 Ma (Fig. 2b, blue stippled line). However, the linear trend
152 should be treated with caution because for older times the polygons containing oceanic areas
153 became less well constrained. At 150 Ma the world uncertainty is $\sim 60\%$ using
154 reconstructions that are based on a reasonably constrained Pangea undergoing breakup while
155 surrounded by simplified oceanic areas in which little is known. Possible additional plate
156 boundaries (like intra-oceanic subduction and adjacent back-arc spreading) are missing from
157 this oceanic realm. Removing this linear trend leads to an average NR of around $0.12^\circ/\text{Myr}$
158 for the past 150 Ma.

159

160 Another indication that this linear trend is an artifact while the average estimated NR is more
161 robust comes from separate analyses of net rotation: for subducted plates only, for oceanic
162 subducted plates only, and for corresponding complementary sets of plates (Fig. 5). We find
163 that for recent times (last 20-30 Ma) net rotations for subducted plates only, and in particular
164 for oceanic subducted plates only, are larger and around a similar axis as for all plates. Net

165 rotations for the complementary sets (plates that are not subducted, and in particular non-
166 oceanic plates) are smaller and around different axes – even close to opposite (angle nearly
167 180°) for the most recent time interval for plates that are not oceanic subducted. This is
168 precisely what we expect from the dynamics of subduction: subducted slabs primarily pull
169 the plates which they are attached to, but, through viscous coupling, also pull the overriding
170 plates towards the trench. For times before about 40 Ma, on the other hand, net rotation for
171 all subsets of plates tend to be around similar axes (small angles in Fig. 5b) which is contrary
172 to expectations from dynamics and therefore again indicates shortcomings in the reference
173 frame. In fact the slope of the dashed blue line in Fig. 2b (around $0.05^\circ/\text{Myr}/50\text{ Myr}$)
174 indicates that around 50 Ma the “artificial” net rotation becomes similar **in magnitude** to the
175 net rotation of the plates that are not subducted or not oceanic subducted (i.e. the sets of
176 plates complementary to ‘oceanic and subducted’); this explains why around this time the
177 transition from the “realistic case” with roughly opposite net rotation to the “unrealistic case”
178 with similar net rotation of the not-subducted (or not oceanic subducted) plates occurs.

179

180 Some of the short-term fluctuations and changes could be real. For the last 50 My we notice
181 a general increase from $0.08^\circ/\text{My}$ (well within the range of geodynamic modeling results) to
182 **$0.13\text{-}0.14^\circ/\text{Myr}$** , which can be attributed to a steadily growing and accelerating Pacific plate
183 at the expense of a shrinking and decelerating Farallon plate (Fig. 2a) and subduction of the
184 Izanagi plate. The Eocene burst of subduction initiation in the western Pacific (Gurnis et al.
185 2004) favored increased driving forces on the Pacific toward the west that may have
186 contributed to the progressively increasing NR since 50 Ma. We conclude that the westward
187 drift is real but only pronounced for the past 30 My and caused by the large and fast Pacific
188 oceanic plate.

189

190 The magnitude of the velocity for a few selected plates is shown in Figure 2a. In addition to
191 the purely oceanic Pacific and Farallon plates we also show the velocity field evolution for
192 Africa (mostly continental and shown as a bar graph since it is our main reference plate) and
193 the Indian plate where the ratio of continental vs. oceanic area has varied substantially
194 through time (see Fig. 1a-d). During the Mid to Late Cretaceous separation of India and the
195 Seychelles from Madagascar (Torsvik et al. 2000), the Indian plate accelerated to speeds of
196 more than 15 cm/year (60-50 Ma) followed by a rapid decrease (50-40 Ma) to ~ 5 cm/year
197 after collision with Eurasia. This is the largest known acceleration/deceleration and is clearly

198 reflected in NR calculations that show a peak between 60-50 Ma ($0.33^\circ/\text{Ma}$). However, this
 199 peak is significantly smaller than present day values estimated from the HS3 model. In order
 200 to explore the significance of this peak we also tested two other Indo-Atlantic plate models
 201 (maintaining the same Pacific model), a fixed hotspot model and a different moving hot spot
 202 model (Fig. 2b). We notice that the 60-50 Ma peak is visible in all reference frames but
 203 somewhat subdued compared with our model. **Any earlier fluctuations differ among the**
 204 **different reference frames; deviations from the linear trend generally do not exceed errors in**
 205 **net rotation inferred from that trend, and are hence not considered robust model features. For**
 206 **a consistent treatment, changing the reference frame in the Pacific and/or African hemisphere**
 207 **also implies changing plate boundaries accordingly. In our online supplement, we hence also**
 208 **include a program that, from a given plate boundary set (also supplied online) that is**
 209 **consistent with the Africa and Pacific rotations given in Table 1, computes boundaries**
 210 **consistent with different absolute rotations for these two plates, while relative rotations**
 211 **within the Pacific and African hemispheres remain the same.**

212

213 **4. Conclusions and future outlook**

214 We have used an improved model of digital plate boundaries and absolute plate motions
 215 through time to compute net lithosphere rotation (NR). We draw the following conclusions:

216

- 217 1. NR with respect to the mantle has been $\sim 0.13^\circ/\text{My}$ for the past 5 My and $0.11 \pm 0.03^\circ/\text{My}$
 218 for the past 50 My.
- 219 2. NR is approximately westward (~ 1.5 cm/yr), but only for the past 30 My (Figs. 3-4). It is
 220 currently dominated by Pacific plate motion.
- 221 3. NR has increased from $\sim 0.08^\circ/\text{My}$ during the past 50 My (Fig. 2b). That we attribute to a
 222 steadily growing/accelerating Pacific plate.
- 223 4. NR magnitudes are three times lower than the HS3 model (Gripp & Gordon 2002) and we
 224 recommend that this model, which differs from all other published hotspot and mantle
 225 models, should be used with caution (at least in the Indo-Atlantic domain).
- 226 5. NR show a pronounced peak ($0.33^\circ/\text{My}$) between 60 and 50 Ma. We consider that this
 227 peak in NR was caused by the Indian plate accelerating to speeds of more than 15
 228 cm/year followed by a rapid deceleration after India collided with Eurasia (5 cm/yr).

229

230 NR fluctuates and gradually increases back in time, and by removing a linear time-trend in
231 the data (Fig. 2b), averages to $\sim 0.12^\circ/\text{Myr}$ for the past 150 Myr. **However, the oceanic area**
232 **reconstructions rely on few constraints and many assumptions for older time intervals; about**
233 **60% of the lithosphere have been subducted since 150 Ma and plate motions are uncertain for**
234 **this fraction.** To realistically reconstruct the proto-Pacific through time, information about
235 the oceanic crust consumed by subduction is needed. Subducted material is imaged by
236 tomographic models (e.g. van der Meer et al. 2010) and we envisage that the next generation
237 of global plate reconstructions and plate boundaries will incorporate at least the first order
238 estimate of the amount of subducted material based on tomography and iterative plate
239 reconstructions.

240

241 **Acknowledgements**

242 We thank Giampiero Iaffaldano for stimulating one of us (THT) to gain interest in developing
243 a revised model of global digital palaeo-plate boundaries, Kevin Burke, **Yanick Ricard**
244 **(Editor) and three anonymous referees for comments**, and Statoil and the Norwegian
245 Research Council for financial support (GPlates Project).

246

247 **References**

- 248 Alvey, A., Gaina, C., Kuszniir, N.J., Torsvik, T.H., 2008. Integrated Crustal Thickness
249 Mapping & Plate Reconstructions for the High Arctic. *Earth Planet. Sci.* 274, 310-321.
- 250 **Argus, D.F., Gordon, R.G., 1991. No-net-rotation model of current plate velocities**
251 **incorporating plate motion model NUVEL-1. *Geophys. Res. Lett.* 18, 2039–2042.**
- 252 Becker, T.W., 2006. On the effect of temperature and strain-rate dependent viscosity on
253 global mantle flow, net rotation, and plate-driving forces. *Geophys. J. Int.* 167, 943-957.
- 254 Becker, T.W., 2008. Azimuthal seismic anisotropy constrains net rotation of the lithosphere.
255 *Geophys. Res. Lett.* 35, doi:10.1029/2007GL032928.
- 256 Bird, P., 2003. An updated digital model of plate boundaries. *Geochem. Geophys. Geosyst.* 4,
257 1027, doi:10.1029/2001GC000252.
- 258 Boyden, J.R., Müller, R.D., Gurnis, M., Torsvik, T.H., Clark, J., Turner, M., Ivey-Law, H.,
259 Watson, R., Cannon, J., 2010. Next-Generation Plate-Tectonic Reconstructions using
260 GPlates. *Geoinformatics*, eds. Randy Keller and Chaitan Baru, Cambridge University Press
261 (in press).

- 262 Čadek, O., Ricard, Y., 1992. Toroidal/poloidal energy partitioning and global lithospheric
263 rotation during Cenozoic time. *Earth Planet. Sci. Lett.* 109, 621-632.
- 264 Doglioni, C., Green, D.H., Mongelli, F., 2005. On the shallow origin of hotspots and the
265 westward drift of the lithosphere. *Geol. Soc. Am. Spec. Paper* 388, 735-749.
- 266 Duncan, R.A., Clague, D.A., 1985. Pacific plate motion recorded by linear volcanic chains, in
267 *The Ocean Basins and Margins, vol.7a, The Pacific Ocean*, edited by A. E. M. Nairn, F. G.
268 Stehli, and S. Uyeda, pp. 89–121, Plenum, New York.
- 269 Funiciello, F., Facenna, C., Heuret, A., Lallemand, S., Di Giuseppe, E., Becker, T.W., 2008.
270 Trench migration, net rotation and slab-mantle coupling. *Earth Planet Sci. Lett.* 271, 233-
271 240.
- 272 Gaina, C., Roest, W., Müller, R.D., 2002. Late Cretaceous-Cenozoic deformation of northeast
273 Asia. *Earth Plan. Sci. Lett.* 197, 273-286
- 274 Gaina, C., Gernigon, L., Ball, P., 2009. Paleocene-Recent Plate Boundaries in the NE
275 Atlantic and the formation of Jan Mayen microcontinent, *J. Geol. Soc. London* 166, 601-
276 616.
- 277 Gaina, C., Müller, R.D., 2007, Cenozoic tectonic and depth/age evolution of the Indonesian
278 gateway and associated back-arc basins. *Earth Sci. Rev.* 83, 177-203.
- 279 Gaina, C., Müller, R.D., Royer, J.-Y., Stock, J., Hardebeck, J., Symonds, P., 1998, The
280 tectonic history of the Tasman Sea: A puzzle with thirteen pieces. *J. Geophys. Res.* 103,
281 12413-12433.
- 282 Gripp, A., Gordon, R.G., 2002. Young tracks of hotspots and current plate velocities.
283 *Geophys. J. Int.* 150, 321-361.
- 284 Gordon, R.G., Jurdy, D.M., 1986. Cenozoic global plate motions. *J. Geophys. Res.* 91, 12
285 389–12 406.
- 286 Gurnis, M., Hall, C., Lavier, L., 2004, Evolving force balance during incipient subduction.
287 *Geochem. Geophys. Geosys.* 5, Q07001, doi:10.1029/2003GC00068.
- 288 Gurnis, M., Turner, M., DiCaprio, L., Spasojevic, S., Müller, R.D., Boyden, J., Seton, M.,
289 Manea, V.C., Bower, D.J., 2010. Global plate reconstructions with continuously closing
290 plates. *Geochem. Geophys. Geosys.* (in review).
- 291 Husson, L., Conrad, C.P., Facenna, C., 2008. Tethyan closure, Andean Orogeny, and
292 westward drift of the Pacific Basin. *Earth Planet. Sci. Lett.* 271, 303-310.
- 293 Heine, C., Müller, R.D, Gaina, C., 2004. Reconstructing the Lost Eastern Tethys Ocean
294 Basin: Convergence history of the SE Asian margin and marine gateways, in *Continent-*

- 295 *Ocean Interactions in the East Asian Marginal Seas*, American Geophysical Union
296 Monograph, pp. 37-54.
- 297 Kreemer, C., 2009. Absolute plate motions constrained by shear wave splitting orientations
298 with implications for hot spot motions and mantle flow. *J. Geophys. Res.* 114, B10405,
299 doi:10.1029/2009JB006416.
- 300 Kreemer, C., Holt, W.E., 2001. A no-net-rotation model of present-day surface motions.
301 *Geophys. Res. Lett.* 28, 4407–4410.
- 302 Le Pichon X., 1968. Sea-floor spreading and continental drift. *J. Geophys. Res.* 73, 3661-97.
- 303 Lithgow-Bertelloni, C., Richards, M.A., Ricard, Y., O'Connell, R.J., Engebretson, D.C.,
304 1993. Toroidal-poloidal partitioning of plate motions since 120 Ma. *Geophys. Res. Lett.* 20,
305 375-378.
- 306 McKenzie, D.P., Parker, R.L., 1967. The North Pacific: An example of tectonics on a sphere.
307 *Nature* 216, 1276-80.
- 308 Morgan, W.J., 1968. Rises, trenches, great faults and crustal blocks. *J. Geophys. Res.* 73,
309 1959-1982.
- 310 Morgan, W.J., Morgan, J.P., 2007. Plate velocities in the hotspot reference frame. *Geol. Soc.*
311 *Am. Spec. Paper* 430, 65-78.
- 312 Müller, R.D., Sdrolias, M., Gaina, C., Roest, W., 2008. Age, spreading rates and spreading
313 asymmetry of the world's ocean crust. *Geochemistry Geophysics Geosystems*, 9, Q04006,
314 doi:10.1029/2007GC001743.
- 315 O'Connell, R.J., Gable, C.W., Hager, B.H., 1991. Toroidal-poloidal partitioning of
316 lithospheric plate motions, in *Glacial Isostasy, Sea-Level and Mantle Rheology*, edited by
317 R. Sabadini, Kluwer Academic Publishers, 535–551.
- 318 O'Neill, C., Müller, R.D., Steinberger, B., 2005. On the uncertainties in hot spot
319 reconstructions and the significance of moving hot spot reference frames. *Geochem.*
320 *Geophys. Geosyst.* 6, Q04003, doi:10.1029/2004GC000784.
- 321 Ricard, Y., Doglioni, C., Sabadini, R., 1991. Differential Rotation Between Lithosphere and
322 Mantle: A Consequence of Lateral Mantle Viscosity Variations. *J. Geophys. Res.* 96, 8407–
323 8415.
- 324 Steinberger, B., Gaina, C., 2007. Plate tectonic reconstructions predict part of Hawaiian
325 hotspot track to be preserved in Bering Sea. *Geology* 35, 407-410.
- 326 Steinberger, B., Torsvik, T.H., 2008. Absolute plate motions and true polar wander in the
327 absence of hotspot tracks. *Nature* 452, 620-623.

- 328 Torsvik, T.H., Tucker, R.F., Ashwal, L.D., Carter, L.M., Jamtveit, B., Vidyadharan, K.T.,
329 Venkataramana, P., 2000. Late Cretaceous India-Madagascar fit and timing of break-up
330 related magmatism. *Terra Nova* 12, 220-224.
- 331 Torsvik, T.H., Müller, R.D., Van der Voo, R., Steinberger, B., Gaina, C., 2008a. Global Plate
332 Motion Frames: Toward a unified model. *Rev. Geophys.* 46, RG3004,
333 doi:10.1029/2007RG000227.
- 334 Torsvik, T.H., Gaina, C., Redfield, T.F., 2008b. Antarctica and Global Paleogeography: From
335 Rodinia, through Gondwanaland and Pangea, to the birth of the Southern Ocean and the
336 opening of gateways. In Cooper, A. K., P. J. Barrett, H. Stagg, B. Storey, E. Stump, W.
337 Wise, and the 10th ISAES editorial team (eds.) *Antarctica: A Keystone in a Changing*
338 *World. Proceedings of the 10th International Symposium on Antarctic Earth Sciences.*
339 Washington, DC: The National Academies Press, 125-140
- 340 Torsvik, T.H., Rouse, S., Labails, C., Smethurst, M.A., 2009. A new scheme for the opening
341 of the South Atlantic Ocean and dissection of an Aptian Salt Basin. *Geophys. J. Intern.* 177,
342 1315-1333.
- 343 van der Meer, D.G., Spakman, W., van Hinsbergen, D.J.J., Amaru, M.L., Torsvik, T.H.,
344 2010. Towards absolute plate motions constrained by lower-mantle slab remnants. *Nature*
345 *Geoscience*, DOI:10.1038/NGEO708.
- 346 Wang, S., Wang, R., 2001. Current plate velocities relative to hotspots: implications for
347 hotspot motion, mantle viscosity and global reference frame. *Earth Planet. Sci. Lett.* 189,
348 133-140.
- 349 Wilson, J.T., 1966. Did the Atlantic close and then reopen? *Nature* 211, 676-681.

350 **Table 1** Absolute motions for the African and Pacific plates. African (Plate 701) motions
 351 are in an Indo-Atlantic mantle (moving hotspot) frame after 100 Ma (O'Neill et al. 2005) and
 352 a TPW corrected palaeomagnetic frame before that (Torsvik et al. 2008a; Steinberger &
 353 Torsvik 2008). Pacific (Plate 901) motions are based on a mantle (moving hotspot) frame
 354 back to 83 Ma (Steinberger & Gaina, 2008) and then a fixed hotspot frame back to 150 Ma
 355 (Duncan & Clague 1985).

Age (Ma)	Indo-Atlantic (Africa)			Pacific		
	Lat.(°)	Long.(°)	Angle(°)	Lat.(°)	Long.(°)	Angle(°)
10	46.2	-87.9	-1.9	72.6	-63.7	8.5
20	45.2	-78.6	-4.0	72.6	-63.7	17.0
30	43.5	-69.7	-6.1	71.1	-62.1	23.4
40	44.6	-54.3	-8.1	68.7	-60.1	27.7
50	37.0	-58.9	-10.3	65.0	-63.4	31.4
60	23.7	-42.1	-12.5	57.2	-72.5	34.0
70	20.7	-39.1	-13.8	53.6	-73.8	35.7
80	17.7	-36.1	-15.0	51.1	-74.0	37.3
90	14.6	-33.3	-16.2	49.1	-74.9	41.7
100	14.4	-29.6	-20.1	47.6	-76.0	47.3
110	6.6	330.5	-26.8	51.4	-74.1	50.8
120	6.1	334.9	-30.5	54.7	-72.1	54.5
130	5.9	334.6	-33.8	57.5	-70.1	58.3
140	7.6	334.1	-38.5	60.0	-68.1	62.3
150	10.3	332.3	-37.3	62.2	-66.0	66.4

356

357 **Table 2** Net rotation calculations.

Time (Ma)	Net Rotation (°/My)	Latitude (°)	Longitude (°)
*5-0	<i>0.13</i>	<i>-67.5</i>	<i>132.1</i>
*10-0	<i>0.14</i>	<i>-69.3</i>	<i>122.5</i>
*20-10	0.15	<i>-77.0</i>	<i>109.8</i>
*30-20	0.10	<i>-61.5</i>	<i>103.2</i>
40-30	0.10	<i>-14.1</i>	<i>94.2</i>
50-40	0.08	<i>19.5</i>	<i>17.6</i>
60-50	<i>0.33</i>	<i>-6.5</i>	<i>33.7</i>
70-60	0.16	18.9	70.1
80-70	0.18	2.8	114.1
90-80	0.32	-30.3	101.0
100-90	0.28	-10.8	94.9
110-100	0.30	-54.4	-21.8
120-110	0.25	-34.4	63.2
130-120	0.24	-25.6	-12.4
140-130	0.25	-8.7	-5.6
150-140	0.23	-5.8	115.3

358 *Pronounced Westward drift

359

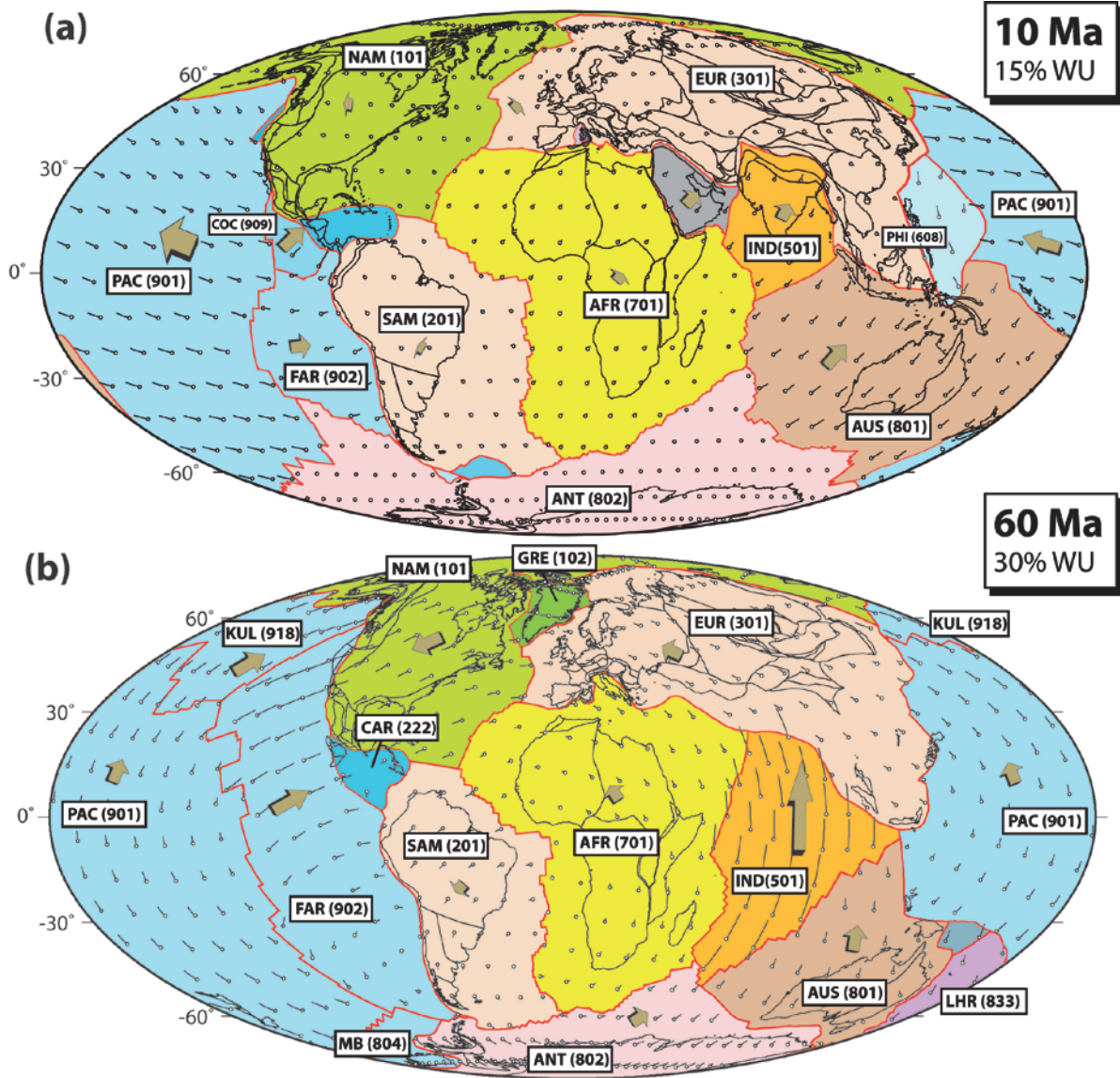


Figure 1 (Torsvik et al.)

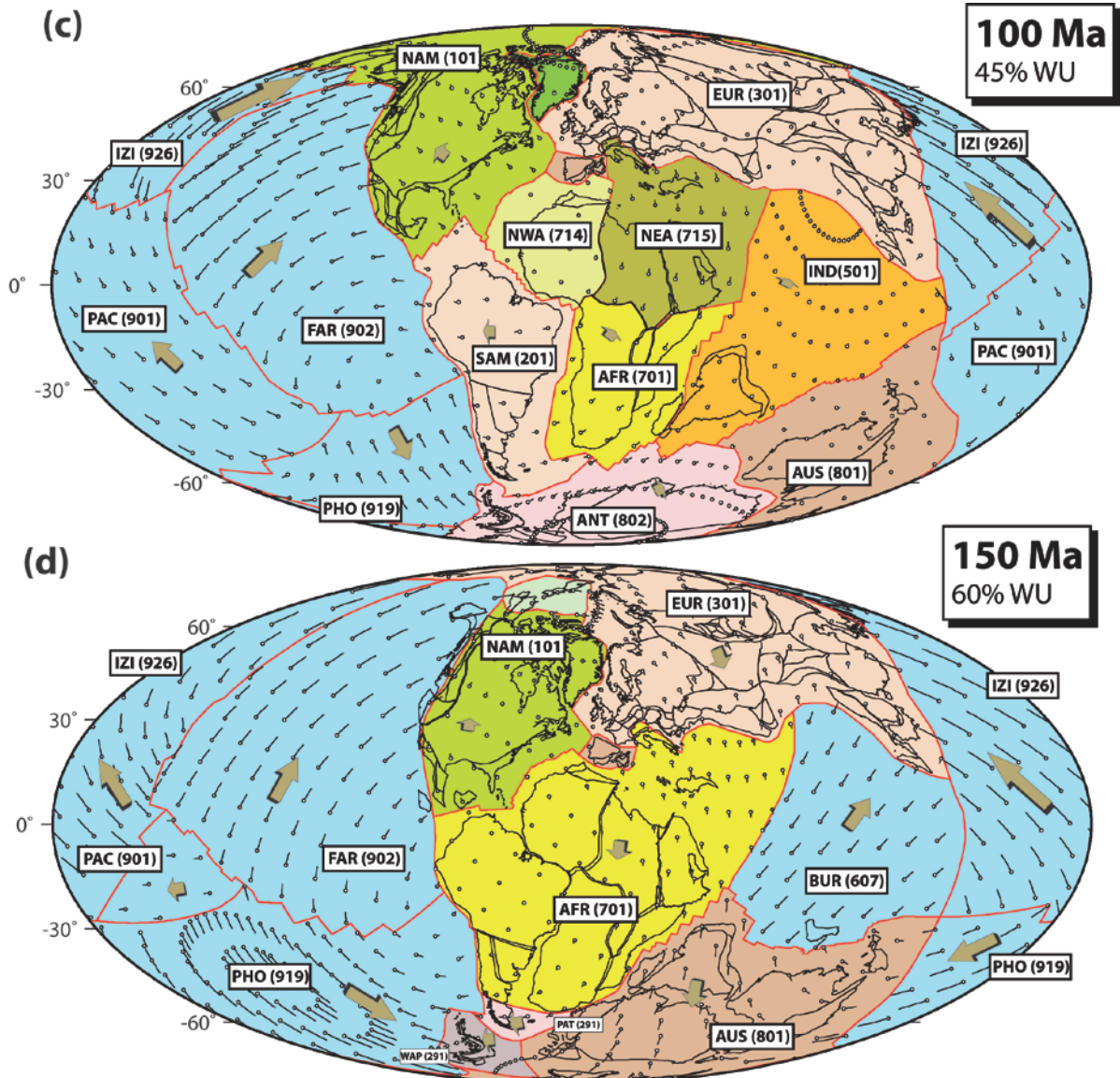
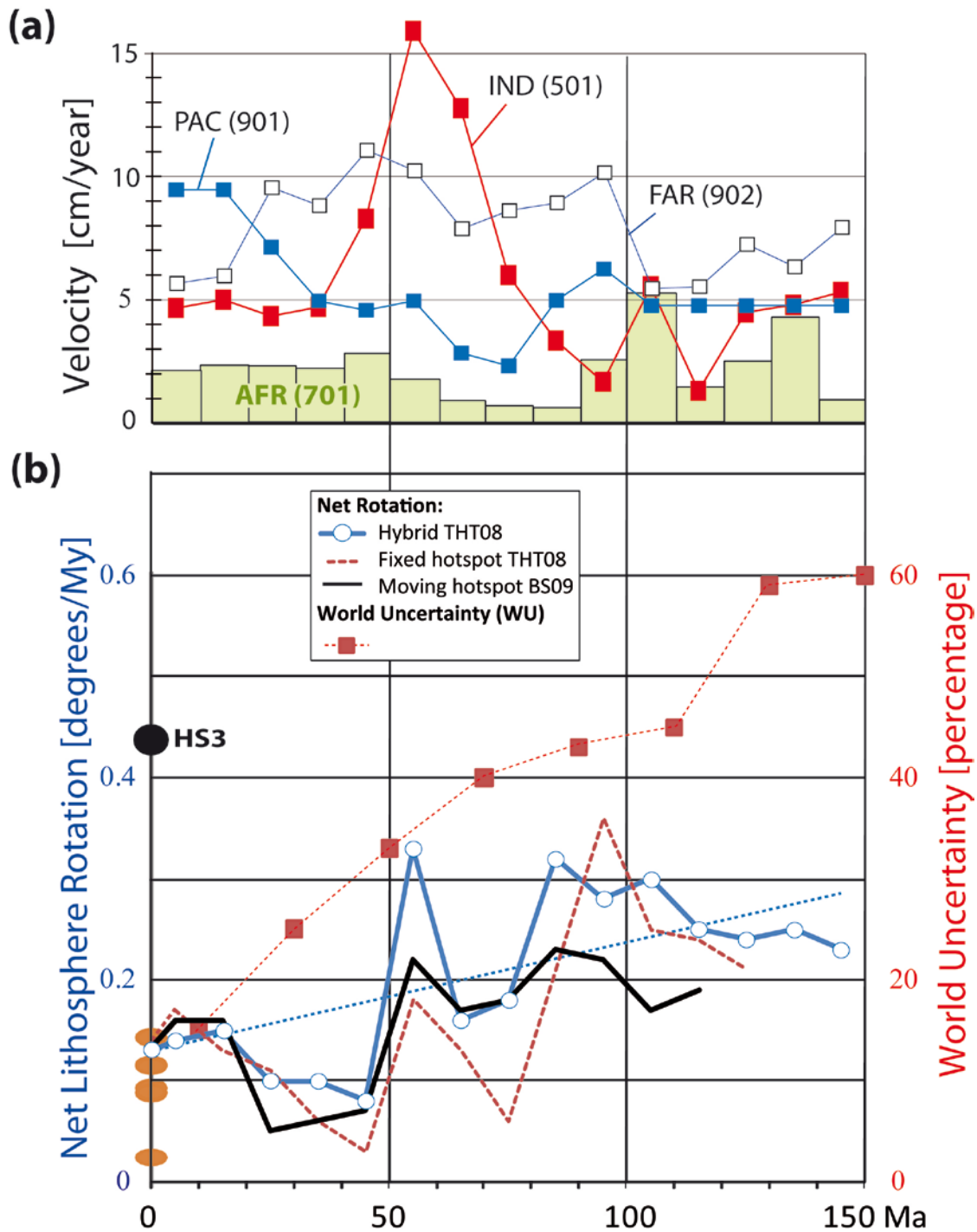


Figure 1 continued (Torsvik et al.)

361

362 **FIGURE 1** Global plate reconstructions and plate polygons (red lines) at 10, 60, 100 and 150
 363 Ma. Dominantly Oceanic plates are shaded blue. Absolute velocity fields are projected 5 My
 364 forward from the reconstructed age. Exaggerated (brown) arrows show the generalized
 365 velocity pattern. WU=world uncertainty. We also show as black lines the continental part of
 366 the plates, mostly present coastlines and intra-plate boundaries that were active at various
 367 times through the Phanerozoic. Extended continental margins are not distinguished.
 368 NAM=North America, EUR=Europe, IND=India, AFR=South Africa, NWA=Northwest
 369 Africa, NEA=Northeast Africa, SAM=South America, PAT=Patagonia, WAT=West
 370 Antarctica, MB=Marie Byrdland, AUS=Australia, ANT=East Antarctica, GRE=Greenland,
 371 PAC=Pacific, FAR=Farallon, COC=Cocos, PHO=Phoenix, KUL=Kula, CAR=Caribbean,
 372 BUR=Burma, PHI=Philippine, LHR=Lord Howe Rise. Mollweide projection.



373

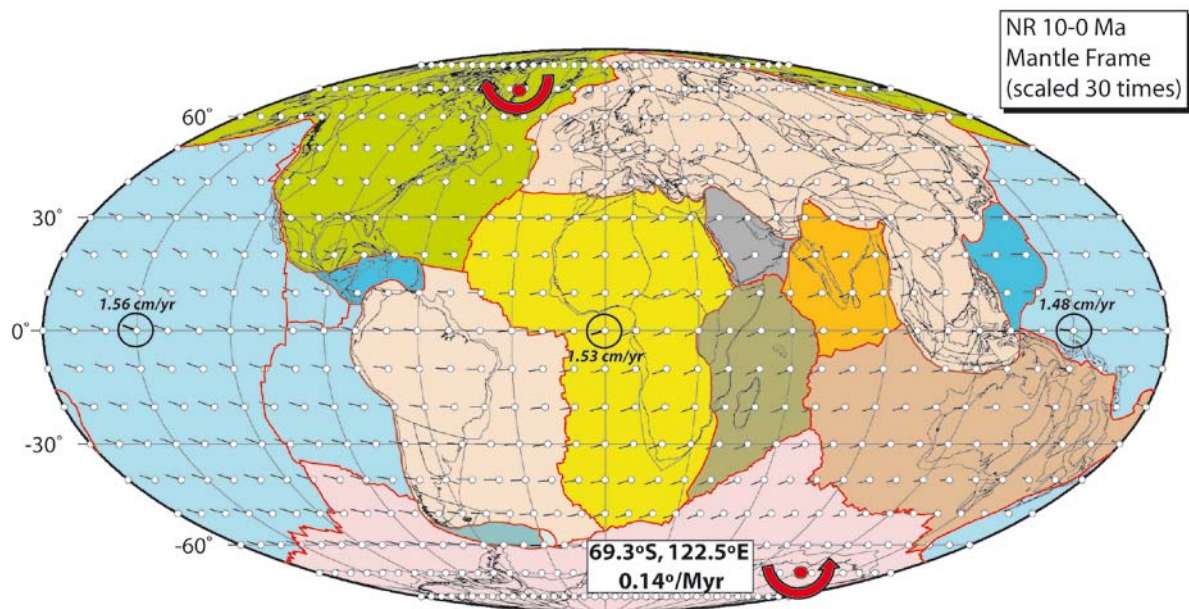
374

Figure 2 (Torsvik et al.)

375 **FIGURE 2** (a) Absolute point velocity for some selected plates, Africa (AFR: 5°S, 15°E),
 376 Pacific (PAC: 0°, 200°E), India (IND:15°N, 75°E) and Farallon (FAR:20°S, 270°E) (b) Net
 377 lithosphere rotation (NR) calculated from our plate polygons and reference frames and
 378 estimated world uncertainty (WU in %), i.e. essentially the fraction of lithosphere subducted

379 **since that time.** NR shows fluctuations and a gradual increase with time (see fitted linear
 380 trend in **stippled** blue for the hybrid TPW corrected plate model; Hybrid THT08). The latter
 381 we relate to increasing WU ('making up more and more' of oceanic plates). NR for the past
 382 150 Ma probably averages to $0.12^\circ/\text{Ma}$. For comparison we also show a fixed hotspot model
 383 for the last 130 Ma (Torsvik et al. 2008a) and a revised global moving hotspot frame (BS09)
 384 based on the New England, Tristan and Reunion hotspots in the African hemisphere (work in
 385 progress). Orange ovals are the range of NR values calculated from geodynamic models
 386 (Becker 2006, *table 4*). Black circle marked HS3 is the NR value ($0.44^\circ/\text{Myr}$) calculated from
 387 the fixed hot spot model of Gripp & Gordon (2002).

388



389

Figure 3 (Torsvik et al.)

390 **FIGURE 3** Net rotation velocity field ($10 \times 10^\circ$ grid) from 10 Ma to present. Because the
 391 counterclockwise net rotation pole is at high southerly latitudes (69.3°S , 122.5°E) this results
 392 in westward drift. We calculate the total vector velocity at three equatorial locations (1.48-
 393 1.56 cm/year; vectors with black circles). The NR velocity field is draped on a simplified
 394 present day plate polygon model. Mollweide projection.

395

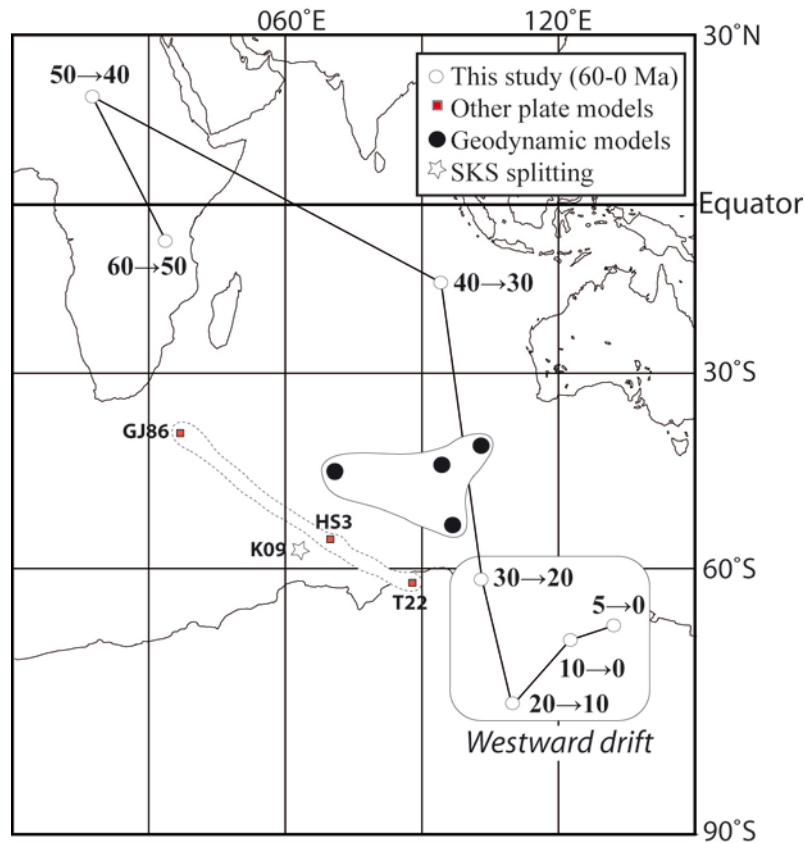


Figure 4 (Torsvik et al.)

396

397

398 **FIGURE 4** NR Euler poles for the past 60 My (Table 2) compared with Euler poles from
 399 some other plate tectonic (GJ86, Gordon & Jurdy 1986; HS3, Gripp & Gordon 2002; T22,
 400 Wang & Wang 2001), and geodynamic models (Becker 2006, table 4) and inferred from SKS
 401 splitting (K09, Kreemer 2009). From our analysis westward drift is only pronounced for the
 402 last 30 Myr. Galls projection.

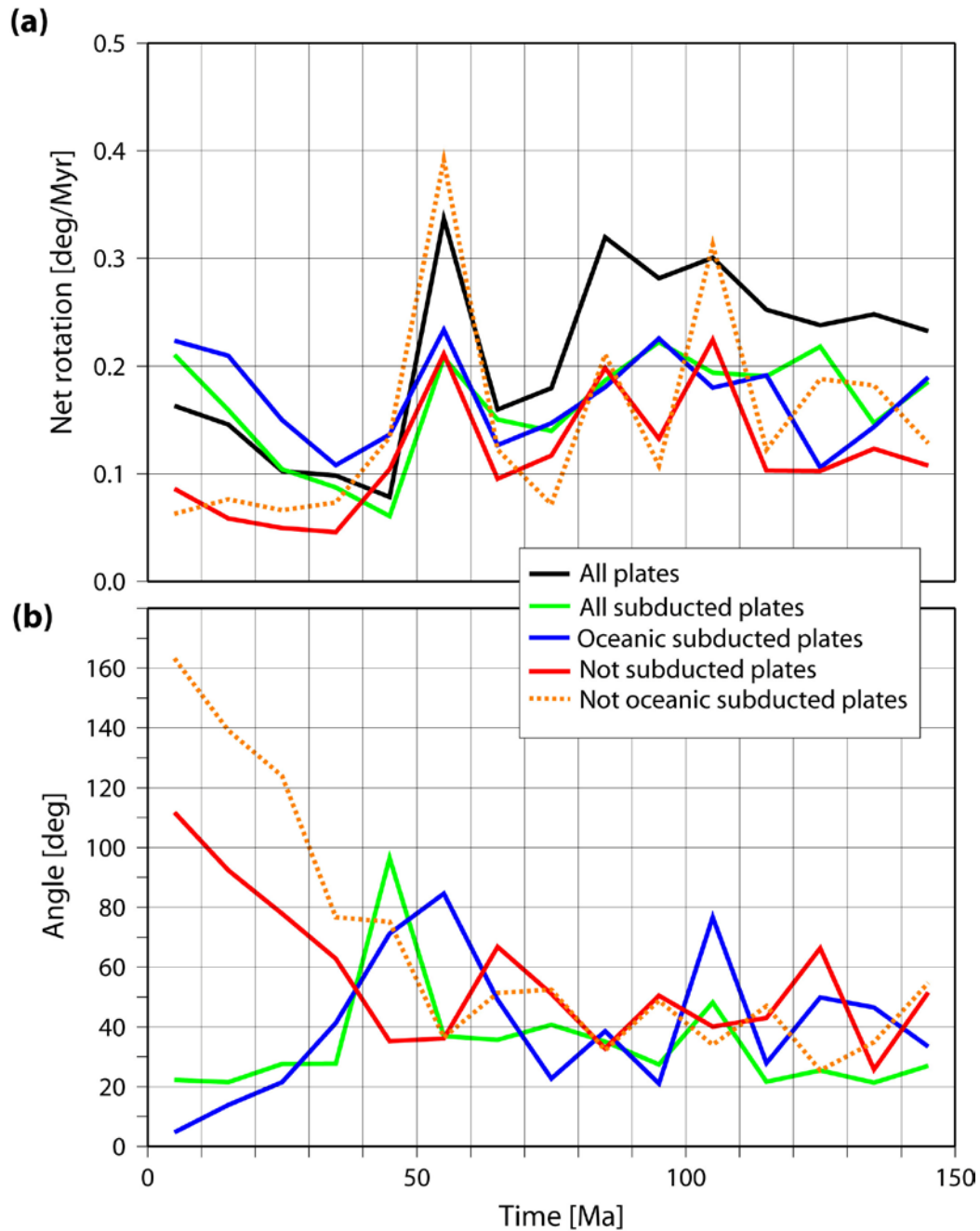


Figure 5 (Torsvik et al.)

403

404

405 **FIGURE 5** Net rotations for subsets of plates. (a) NR for all plates (black), for all subducted
 406 plates (green), for oceanic subducted plates (blue), for not subducted plates (red;
 407 complementary set to green) and for not oceanic subducted plates (stippled orange;
 408 complementary to blue). (b) Angle between the axes of net rotation for all plates, and the
 409 same subsets of plates as in (a), with same color codes.

410

411 **Supplementary Materials**

412 Digital reconstructed plate boundaries (0-150 Ma), stage poles (Filename:
 413 *0_150_StagePoles.dat*) averaged over 10 Myr (e.g. stage pole at 20 Ma is calculated from 20
 414 to 10 Ma) and a Fortran program (Filename: *bplates.f*) that re-computes the plate boundaries
 415 for different absolute rotations than given in Table 1), can be downloaded at
 416 <http://www.geodynamics.no/poly/PlateTectonics.zip>. Stage poles are also listed below
 417 (Table S1) followed by a brief description of *bplates.f*. Digital plate boundaries are provided
 418 in two different file formats: (1) Standard 'PLATES' ASCHII format (filename:
 419 *0_150_Reconstructed.dat*) and (2) Arc-Gis Shape format (three files named:
 420 *0_150_Reconstructed.shp*, *0_150_Reconstructed.shx*, *0_150_Reconstructed.DBF*).

421

422 **Table S1:** Stage Poles

Time	Latitude	Longitude	ω ($^{\circ}$/Myr)	PlateId (Name)
10	6.08	-37.65	0.48	840 (Aluk)
10	84.00	130.58	0.16	820 (Scotia)
10	51.17	-170.38	0.15	802 (Antarctica)
10	25.31	42.52	0.58	801 (Australia)
10	37.92	-100.31	0.60	902 (Farallon)
10	51.60	14.71	-0.19	201 (Amazonia)
10	3.74	40.01	-0.12	224 (Caribbean)
10	18.20	-107.00	1.97	909 (Cocos)
10	25.42	151.97	-1.25	608 (Philippine Sea)
10	51.31	-11.74	0.42	503 (Arabia)
10	40.39	14.55	0.50	501 (India)
10	46.19	-87.86	0.19	701 (South Africa)
10	17.70	13.98	-1.32	322 (Calabria)
10	38.76	-140.30	0.16	306 (Corsica-Sardinia)
10	20.25	-81.77	-0.25	903 (Juan de Fuca)
10	72.61	-63.73	-0.85	901 (Pacific)
10	38.76	-140.30	0.16	301 (Europe)
10	36.90	76.50	-0.19	101 (North America)
20	4.66	-37.93	0.56	840 (Aluk)
20	32.47	-8.05	-0.13	820 (Scotia)
20	62.10	-117.82	0.13	802 (Antarctica)
20	11.12	-127.40	-0.34	847 (Solomon)
20	77.57	170.91	0.57	902 (Farallon)
20	20.21	171.41	-0.92	688 (SW Caroline Basin)
20	28.04	24.46	0.58	801 (Australia)
20	52.77	1.76	-0.25	201 (Amazonia)
20	21.56	23.96	-0.15	224 (Caribbean)

20	29.29	-127.45	1.73	909 (Cocos)
20	12.99	154.53	-1.66	608 (Philippine Sea)
20	12.28	155.44	-2.02	659 (Izu-Bonin-Mariana)
20	45.34	-21.58	0.45	501 (India)
20	54.96	-10.93	0.55	322 (Calabria)
20	54.96	-10.93	0.55	306 (Corsica-Sardinia)
20	43.52	-70.47	0.21	701 (South Africa)
20	3.59	103.85	0.24	903 (Juan de Fuca)
20	72.61	-63.73	-0.85	901 (Pacific)
20	44.62	-118.57	0.16	301 (Europe)
20	41.20	88.34	-0.22	101 (North America)
30	15.70	-33.95	0.23	840 (Aluk)
30	56.85	152.08	0.12	804 (Marie Byrdland)
30	40.10	22.82	1.27	838 (NW South Fiji Basin)
30	69.32	144.73	0.10	802 (Antarctica)
30	53.60	48.94	1.04	839 (East South Fiji Basin)
30	33.12	16.83	1.11	847 (Solomon)
30	6.21	134.97	-1.59	688 (SW Caroline Basin)
30	3.56	132.70	-1.35	689 (NE Caroline Basin)
30	9.68	143.96	-1.35	690 (SE Caroline Basin)
30	9.68	143.96	-1.35	653 (NW Caroline Sea)
30	21.95	33.76	0.64	801 (Australia)
30	56.20	-1.61	-0.26	201 (Amazonia)
30	10.36	155.74	-1.90	659 (Izu-Bonin-Mariana)
30	30.64	22.56	-0.15	224 (Caribbean)
30	16.22	150.34	-0.82	608 (Philippine Sea)
30	64.06	-175.95	0.88	902 (Farallon)
30	19.79	33.31	0.66	501 (India)
30	38.13	-54.99	0.21	701 (South Africa)
30	62.65	175.87	1.00	903 (Juan de Fuca)
30	67.26	-56.76	-0.64	901 (Pacific)
30	15.52	-126.82	0.11	301 (Europe)
30	47.38	80.37	-0.21	101 (North America)
40	9.32	-27.44	0.29	840 (Aluk)
40	32.44	136.46	0.20	804 (Marie Byrdland)
40	39.94	113.14	0.12	802 (Antarctica)
40	25.76	37.35	0.54	857 (North Loyalty Basin)
40	43.41	4.59	2.23	847 (Solomon)
40	25.76	37.35	0.54	801 (Australia)
40	4.52	121.25	1.14	645 (Celebes Sea)
40	13.07	-24.77	-0.08	608 (Philippine Sea)
40	6.95	165.29	0.53	665 (North Celebes)
40	72.95	-47.88	-0.25	201 (Amazonia)
40	5.47	-67.48	-0.28	222 (Caribbean)
40	35.56	29.69	0.59	501 (India)

40	16.65	-73.96	-0.55	609 (North Philippine Sea)
40	36.32	-18.16	0.24	701 (South Africa)
40	58.73	129.45	1.00	902 (Farallon)
40	56.75	-48.47	-0.45	901 (Pacific)
40	56.75	-48.47	-0.45	918 (Kula)
40	50.16	97.69	-0.13	102 (Greenland)
40	13.07	-24.77	-0.08	301 (Europe)
40	84.31	104.90	-0.22	101 (North America)
50	35.53	-151.09	0.16	804 (Marie Byrdland)
50	35.96	-137.44	0.14	802 (Antarctica)
50	45.79	-22.46	0.10	801 (Australia)
50	38.42	-64.62	-0.42	901 (Pacific)
50	55.45	56.18	-0.35	201 (Amazonia)
50	32.22	70.29	-0.28	224 (Caribbean)
50	17.75	-12.78	0.77	501 (India)
50	12.17	-71.76	0.26	701 (South Africa)
50	55.97	121.05	1.35	902 (Farallon)
50	32.39	-59.93	-0.92	918 (Kula)
50	26.37	83.44	-0.39	102 (Greenland)
50	20.23	53.48	-0.24	301 (Europe)
50	52.81	85.54	-0.38	101 (North America)
60	5.84	-165.16	-0.43	804 (Marie Byrdland)
60	23.80	-172.19	-0.47	802 (Antarctica)
60	40.57	-129.25	-0.66	833 (Lord Howe Rise)
60	39.38	-93.66	-0.90	836 (Lousiade Plateau)
60	21.23	-169.22	-0.57	801 (Australia)
60	48.38	169.11	-0.62	201 (Amazonia)
60	6.11	-59.57	1.56	222 (Caribbean)
60	0.01	177.76	-1.59	501 (India)
60	17.59	167.05	-0.45	701 (South Africa)
60	1.31	100.29	0.56	901 (Pacific)
60	46.17	108.69	1.41	902 (Farallon)
60	14.93	127.89	1.25	918 (Kula)
60	47.96	144.88	-0.60	102 (Greenland)
60	54.12	165.01	-0.40	301 (Europe)
60	41.78	161.63	-0.69	101 (North America)
70	78.51	96.70	0.18	802 (Antarctica)
70	31.33	-53.09	-0.67	833 (Lord Howe Rise)
70	59.60	49.68	0.18	801 (Australia)
70	79.30	159.06	-0.29	201 (Amazonia)
70	17.78	-2.87	1.21	501 (India)
70	4.29	-69.10	-0.28	901 (Pacific)
70	8.46	161.04	-0.16	701 (South Africa)
70	40.02	-107.58	-1.46	926 (Izanagi)
70	54.22	138.14	0.87	902 (Farallon)

70	10.24	135.76	-0.11	102 (Greenland)
70	74.69	-2.60	-0.16	301 (Europe)
70	79.97	145.36	-0.34	101 (North America)
80	18.98	122.89	0.56	833 (Lord Howe Rise)
80	11.27	147.93	0.27	802 (Antarctica)
80	9.00	133.29	0.24	801 (Australia)
80	73.01	-24.38	-0.51	201 (Amazonia)
80	18.89	10.44	0.60	501 (India)
80	7.98	-62.33	-0.22	901 (Pacific)
80	14.16	165.01	-0.16	701 (South Africa)
80	55.90	151.69	0.90	902 (Farallon)
80	40.36	-110.10	-1.41	926 (Izanagi)
80	71.11	45.51	-0.17	102 (Greenland)
80	78.71	56.90	-0.16	301 (Europe)
80	74.18	-2.72	-0.51	101 (North America)
90	22.29	-48.45	-0.52	802 (Antarctica)
90	20.12	143.88	-0.56	919 (Phoenix)
90	28.85	-56.60	-0.53	801 (Australia)
90	32.34	-73.60	-0.46	901 (Pacific)
90	52.26	-23.09	-0.56	201 (Amazonia)
90	22.51	-138.87	-1.37	501 (India)
90	60.63	6.99	-0.48	305 (Armorica)
90	19.26	168.58	-0.17	701 (South Africa)
90	43.50	120.32	0.97	902 (Farallon)
90	40.48	-107.44	-1.68	926 (Izanagi)
90	62.55	9.32	-0.43	102 (Greenland)
90	60.63	6.99	-0.48	301 (Europe)
90	65.86	0.00	-0.64	101 (North America)
100	69.11	123.42	0.29	802 (Antarctica)
100	9.51	-165.25	-0.75	919 (Phoenix)
100	20.05	87.66	0.16	801 (Australia)
100	10.58	-15.40	0.40	701 (South Africa)
100	61.65	-27.27	-0.34	201 (Amazonia)
100	35.99	-76.01	-0.58	901 (Pacific)
100	28.00	-14.81	0.15	501 (India)
100	10.58	-15.40	0.40	714 (NW Africa)
100	54.40	26.35	-0.38	305 (Armorica)
100	12.23	-16.40	0.41	715 (NE Africa)
100	37.85	115.74	1.08	902 (Farallon)
100	38.97	-106.44	-1.80	926 (Izanagi)
100	60.06	31.12	-0.36	102 (Greenland)
100	54.40	26.35	-0.38	301 (Europe)
100	63.75	24.02	-0.43	101 (North America)
110	37.13	-119.42	0.19	802 (Antarctica)
110	14.41	145.81	-0.74	702 (Madagascar)

110	14.47	165.98	-0.93	919 (Phoenix)
110	84.89	-26.89	-0.30	801 (Australia)
110	14.41	145.81	-0.74	701 (South Africa)
110	64.22	101.08	-0.61	201 (Amazonia)
110	85.01	165.04	-0.48	901 (Pacific)
110	20.87	135.52	-0.51	501 (India)
110	14.41	145.81	-0.74	714 (NW Africa)
110	46.91	95.92	-0.76	304 (Iberia)
110	13.11	145.65	-0.75	715 (NE Africa)
110	52.71	135.03	0.64	902 (Farallon)
110	50.26	102.63	-0.84	102 (Greenland)
110	49.77	-119.16	-1.63	926 (Izanagi)
110	47.38	101.78	-0.81	301 (Europe)
110	53.48	101.13	-0.87	101 (North America)
120	34.54	128.47	0.46	802 (Antarctica)
120	4.84	-178.65	-0.43	702 (Madagascar)
120	17.24	-68.75	-0.50	801 (Australia)
120	14.50	170.65	-0.93	919 (Phoenix)
120	4.84	-178.65	-0.43	701 (South Africa)
120	44.62	-160.55	-0.25	201 (Amazonia)
120	85.01	165.03	-0.48	901 (Pacific)
120	9.40	-157.00	-0.19	501 (India)
120	4.84	-178.65	-0.43	714 (NW Africa)
120	23.47	7.22	2.50	304 (Iberia)
120	2.80	-179.59	-0.44	715 (NE Africa)
120	67.47	76.47	-0.47	102 (Greenland)
120	52.52	139.33	0.64	902 (Farallon)
120	50.18	-114.48	-1.63	926 (Izanagi)
120	64.20	82.98	-0.43	301 (Europe)
120	70.06	69.71	-0.52	101 (North America)
130	72.20	100.92	0.86	803 (Antarctic Peninsula)
130	13.16	-99.12	-0.20	802 (Antarctica)
130	1.93	-138.97	0.21	291 (Patagonia)
130	31.22	-126.66	-0.23	702 (Madagascar)
130	16.41	-128.58	0.18	202 (Parana)
130	1.93	-138.97	0.21	290 (Colorado)
130	7.17	116.11	-1.72	919 (Phoenix)
130	17.06	-99.74	-0.21	801 (Australia)
130	4.70	-28.38	0.33	701 (South Africa)
130	0.10	-83.75	0.22	201 (Amazonia)
130	85.01	165.03	-0.48	901 (Pacific)
130	0.00	114.82	-0.28	714 (NW Africa)
130	29.58	-161.07	-0.97	501 (India)
130	30.38	75.27	-0.46	304 (Iberia)
130	4.84	-28.39	0.33	715 (NE Africa)

130	22.65	96.90	0.68	902 (Farallon)
130	43.00	-115.80	-1.43	926 (Izanagi)
130	8.60	87.25	-0.48	103 (Arctic Alaska)
130	31.01	77.59	-0.47	101 (North America)
130	31.01	77.59	-0.47	301 (Europe)
140	42.68	143.20	-1.07	803 (Antarctic Peninsula)
140	24.65	-33.11	0.33	291 (Patagonia)
140	28.09	-28.27	0.40	202 (Parana)
140	26.36	-30.83	0.36	290 (Colorado)
140	23.84	37.45	0.21	801 (Australia)
140	12.82	121.54	-1.35	919 (Phoenix)
140	12.48	-1.40	0.46	501 (India)
140	85.01	165.03	-0.48	901 (Pacific)
140	20.45	-29.04	0.47	201 (Amazonia)
140	2.26	129.85	-0.41	304 (Iberia)
140	19.71	-25.62	0.49	701 (South Africa)
140	12.97	-25.79	1.40	607 (Burma-Enderby)
140	3.87	129.99	-0.43	101 (North America)
140	20.45	144.13	0.58	902 (Farallon)
140	48.53	-98.98	-1.30	926 (Izanagi)
140	42.29	-46.70	1.32	103 (Arctic Alaska)
140	3.87	129.99	-0.43	301 (Europe)
150	67.59	145.77	-0.75	803 (Antarctic Peninsula)
150	35.30	172.69	0.25	291 (Patagonia)
150	10.46	122.08	0.51	801 (Australia)
150	17.24	125.57	-0.93	919 (Phoenix)
150	85.01	165.03	-0.48	901 (Pacific)
150	0.37	10.16	-0.39	304 (Iberia)
150	47.65	171.27	0.25	701 (South Africa)
150	37.37	-18.56	1.01	607 (Burma-Enderby)
150	3.82	12.46	-0.38	101 (North America)
150	19.38	154.50	0.73	902 (Farallon)
150	66.14	-56.97	2.02	103 (Arctic Alaska)
150	46.93	-97.59	-1.58	926 (Izanagi)
150	2.38	12.51	-0.38	301 (Europe)

423

424

425 **Description of *bplates.f***

426 We supply a routine *bplates.f* that modifies plate boundaries consistent with a change of
427 Africa and Pacific absolute plate rotations, while relative rotations within the Pacific and
428 African hemispheres remain the same. The sample input file *bplates.in* specifies in the first
429 seven lines:

- 430 1. the number of finite rotations per plate
- 431 2. the file with the new Pacific plate rotations, for which the new set of plate boundaries is
 432 created. Rotations need to be given the same way as in Table 1 (age, latitude, longitude,
 433 angle), and ages need to correspond to the input plate boundary file. However, the first
 434 rotation needs to correspond to the first set of boundaries with *non-zero* ages -
 435 boundaries for zero age are left unmodified. Therefore the rotation file should not
 436 contain a first line with zeroes, even though the plate boundary file contains the set of
 437 present-day boundaries. If the number of time intervals before present for which plate
 438 boundaries are given is larger than the number of rotations, then boundaries for time
 439 intervals before the oldest rotation are not rotated.
- 440 3. the file with the new Africa rotations.
- 441 4. the file with the original Pacific rotations (Table 1) used to generate the existing set of
 442 plate boundaries.
- 443 5. the file with the original Africa rotations (Table 1).
- 444 6. The existing file with plate boundaries *0_150_Reconstructed.dat* which is also provided
 445 in this online supplement.
- 446 7. The output file for the modified plate boundaries (given as closed polygons around each
 447 plate; one file for all time intervals, like the input file)

448

449 The remaining lines contain the names of four output files per time interval: First (here
 450 "...d1") for all boundaries in that time interval, then "...d2" for boundaries between two
 451 "African set" plates, "...d3" between two "Pacific set" plates and "...d4" between one "African
 452 set" and one "Pacific set" plate. For each boundary between two plates, the "header" contains
 453 the number of points, the ID numbers of plates on the "left" and "right" side of the boundary,
 454 and secondary plate ID numbers assigned consecutively at each time interval: in case plates
 455 have the same primary ID number in the same time interval, the secondary number is always
 456 unique.

457

458 In brief, the program *bplates.f* performs the following steps:

- 459 • In a "pre-processing", closed polygons around each plate are split up into individual
 460 boundaries between two plates.
- 461 • These boundaries are rotated according to the change from "old" to "new" rotations
 462 (program lines 146-168): Plates are separated into "African" and "Pacific" sets. The

463 "Pacific" set includes all plates with ID # >900. Back to 80 Ma ($i \leq 80$) no Phoenix plate
464 exists in our model, and the "Pacific" set additionally includes plates 802 (Antarctica),
465 804 (Bellinghausen/Marie Birdland) and 840 (Aluk). In the interval 0-10 Ma, it also
466 includes plate 820 (Scotia). Boundaries within the Pacific set are rotated according to
467 Pacific rotations. Boundaries between the Pacific and African sets or within the African
468 set of plates are rotated according to African rotations. This step disconnects plate
469 boundaries within the Pacific set of plates from the "ring" separating the Pacific and
470 African sets.

- 471 • All points of boundaries within the Pacific set, that end up on the African set of plates
472 after the rotations, are removed, in order to avoid boundaries crossing each other.
- 473 • Remaining boundaries within the Pacific set are connected to the closest points on the
474 "ring" surrounding the Pacific set.
- 475 • The "post-processing" re-combines rotated and re-connected boundaries to closed
476 polygons.